Remote Sensing the Impact of Sugarcane Growing on the Land Cover Change of Mabira Forest in Uganda

Ivan Innocent Sekibenga

A Research Project carried out at The School of Geography, Geology, and Environment

University of Leicester

January 2, 2023

Introduction

Background

Mabira Forest (**Figure 1**) is a protected rainforest in Uganda covering approximately 300 square kilometers. It is home to over 300 species of trees and various species of mammals, birds, reptiles, and insects, including chimpanzees, colobus monkeys, forest elephants, and bushbucks. The forest also supports small communities who rely on the forest for their livelihoods, including timber, firewood, and non-timber forest products (Baranga, 2007; Baranga et al., 2013). Mabira Forest is located in the districts of Buikwe, Kayunga, Jinja, and Mukono, about 50 kilometers east of the capital city, Kampala, at latitude 0° 34' 0" North and longitude 32° 57' 0" East.

Mabira Forest has a tropical climate with high humidity and average temperatures ranging from 23 to 27 degrees Celsius. It sits at an altitude of between 1,100 and 1,300 meters above sea level and is bounded by the Nile River to the west and the Ssezibwa River to the east. It is located in the Nile River Basin.

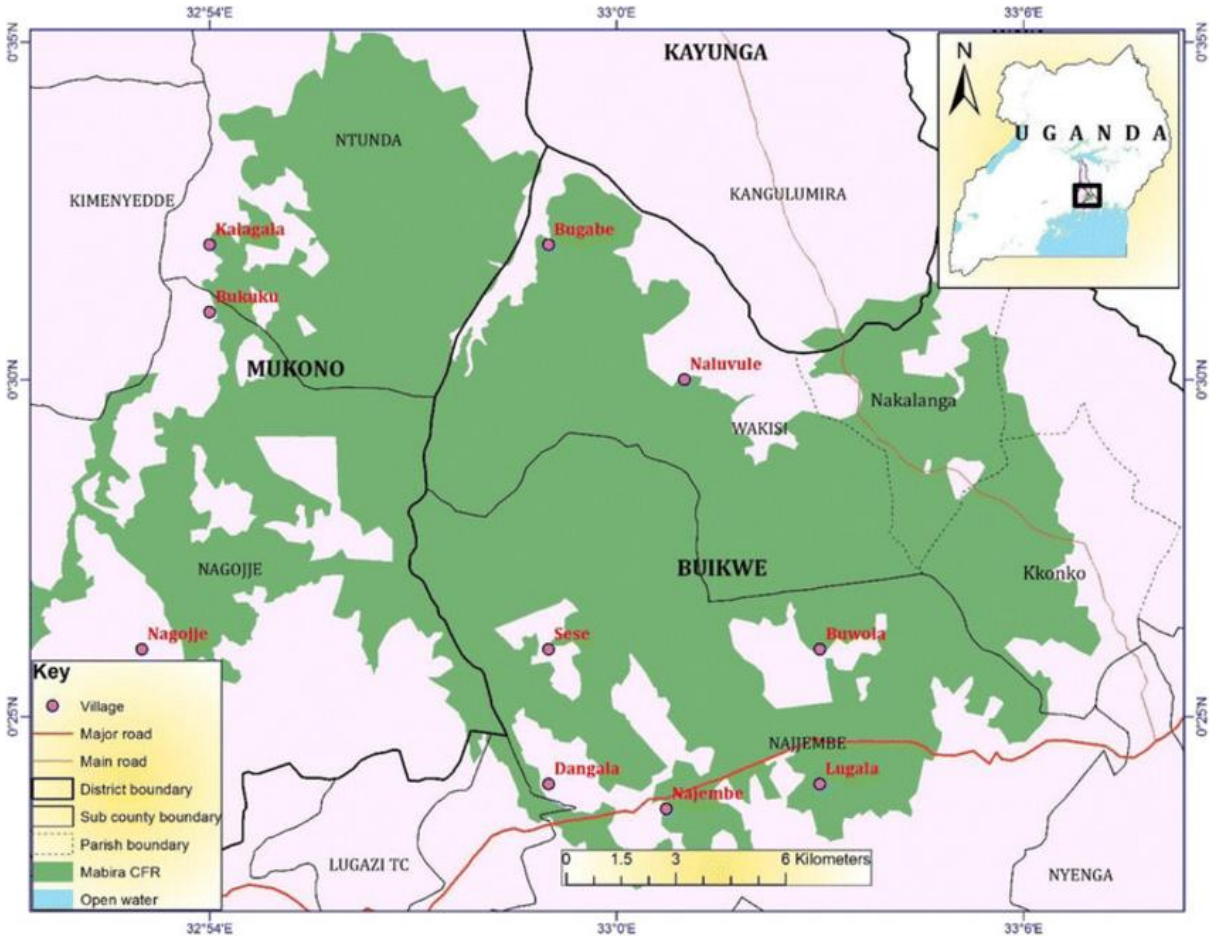

Figure 1: Map showing the land coverage by Mabira Forest in the Buikwe, Mukono and Kayunga districts of Uganda.

Problem Statement:

Mabira Forest in Uganda has experienced threats such as encroachment and illegal logging, particularly the expansion of sugar cane cultivation, which has caused deforestation and habitat loss. The demand for sugar and the growth of the sugar processing industry in Uganda have contributed to this increase in sugar cane production. This cultivation may also lead to competition for water resources between the forest and the crop, potentially impacting the health and survival of the forest's plants and animals (Baranga, 2007; Baranga et al., 2013). Despite efforts by the Ugandan government to protect the forest and prevent illegal activities, the problem of encroachment and land degradation persists in Mabira Forest.

Literature Review

Understanding spatial and land cover changes, and how human activities interact with natural phenomena is crucial for effective land management and decision-making (Rawat & Kumar, 2015).

Mbayaki et al. (2016) used GIS and remote sensing to study land use and land cover change in the Mumias district of Kenya from 1984-2015. Image pre-processing included: image spatial subsetting, radiometric correction, pan sharpening, and image enhancement. They used Landsat satellite images and a supervised classification method with the maximum likelihood algorithm to determine six classes of land use andcover. Error matrix was used to determine the accuracy of each classified image using kappa coefficients, user accuracy, and producer accuracy statistics. They found that maize and sugarcane had the most significant changes with a 54% increase and 39% reduction, respectively.

Tewabe and Fentahun (2020) used Landsat TM images from 1986, 2002, and 2018 to identify land use change in the Lake Tana basin in Ethiopia. Image pre-processing was conducted and consisted of the detection and restoration of bad lines, geometric rectification, radiometric calibration, and atmospheric correction. They used ENVI and ArcGIS software to conduct a supervised classification with the maximum likelihood algorithm and six land cover classes. They assessed the classification accuracy with the kappa coefficient.

Hegazy and Kaloop (2015) studied land use change in Mansoura and Talkha, Egypt from 1985-2010 using Landsat TM images. They performed histogram equalization and used unsupervised and supervised classification with the ISODATA and maximum likelihood algorithms to form four land cover classes. They generated land use change maps and a transition probability matrix, which they used to create a Markov chain model predicting land cover for the cities in 2035.

From the literature review above, this project will instead utilize two higher spatial resolution 10m images from the Sentinel-2 satellite to improve accuracy from Landsat’s 30m resolution used in the reviewed studies. These two images of the spatial extent of Mabira Forest in 2017 and 2019 will undergo supervised classification by the Maximum likelihood algorithm to aid in quantifying and detecting the change in Mabira Forest cover and sugar cane plantation cover in and around Mabira forest. A land cover transition matrix will be generated. The analyzed data will also be presented using thematic maps, tables, and graphs.

Aim

This project aims to use satellite imagery data from Sentinel 2 to study the land cover and land use changes in and around Mabira Forest, specifically focusing on the impact of encroachment and illegal logging on the area of the forest and the effect of sugarcane cultivation on the spatial extent of Mabira Forest.

Methods

Sentinel-2 Satellite:

To choose the best remotely sensed data for image classification, it is crucial to understand the advantages and disadvantages of various types of sensors (Gomez et al., 2016). Sentinel-2 is a satellite mission developed by the European Space Agency (ESA) as part of the Copernicus program. It consists of two satellites, Sentinel-2A and Sentinel-2B, that are designed to provide high-resolution, multispectral imagery of Earth's surface. The satellite sensors are designed to acquire images of the Earth's surface in 13 spectral bands (**Table 1**), with a spatial resolution ranging from 10 to 60 meters, depending on the band.

The spectral resolution of Sentinel-2 refers to the range of wavelengths that the sensors can detect. Sentinel-2 has a spectral resolution of 443-2190 nm, which means that it can detect wavelengths in the visible, near-infrared, and shortwave infrared regions of the electromagnetic spectrum. The temporal resolution of Sentinel-2 refers to the frequency with which the satellite acquires images of the Earth's surface. Sentinel-2 has a temporal resolution of 5 days, which means that it can acquire an image of any given location on Earth once every 5 days. The radiometric resolution of Sentinel-2 refers to the range of brightness values that the sensors can detect. Sentinel-2 has a radiometric resolution of 12 bits per pixel, which means that it can detect 4096 different brightness levels. Overall, the combination of Sentinel-2's spatial, spectral, temporal, and radiometric resolutions makes it a powerful tool for a wide array of applications, including mapping, land cover and land use analysis, environmental monitoring, and disaster response.

BAND NAME	BAND NUMBER	WAVELENGTH (nm)		SPATIAL RESOLUTION(m)
		Sentinel-2A	Sentinel-2B	
Coastal aerosol	1	442.7	442.3	60
Blue	2	492.4	492.1	10
Green	3	559.8	559.0	10
Red	4	664.6	665.0	10
Vegetation Red Edge	5	704.1	703.8	20
Vegetation Red Edge	6	740.5	739.1	20
Vegetation Red Edge	7	782.8	779.7	20
Near Infra-Red (NIR)	8	832.8	833.0	10
Narrow NIR	8A	864.7	864.0	20
Water Vapour	9	945.1	943.2	60
SWIR-Cirrus	10	1373.5	1376.9	60
Short wave Infrared (SWIR)	11	1613.7	1610.4	20
Short wave Infrared (SWIR)	12	2202.4	2185.7	20

Table 1: Table showing the band spectral and spatial resolutions of the Sentinel-2A and Sentinel 2B satellite

Sentinel-2 Satellite Data Acquisition and Image Processing:

Level 2 Sentinel-2 satellite data which was atmospherically corrected was utilized. The projection used is Universal Transverse Mercator, zone 36. World Geodetic System 1984 was used for Spheroid and Datum. European Petroleum Survey (EPSG) Code used is 32636. Satellite imagery level 2A data was downloaded from www.sentinel-hub.com. Two cloud-free images were downloaded dated 25 January 2017 and 16 March 2019, respectively. Of the 13 available bands (**Table 1**), only Blue (2), Green (3), Red (4), and Near-infrared (8) bands were downloaded as 32-bit float TIFF files. Using ERDAS IMAGINE 2016's *Layer Stack* function, two multi-band images were formed for 2017 and 2019 (Khorram and Nelson, 2019). Image sub-setting was carried out using ERDAS IMAGINE to limit and focus the study area to the extent of Mabira forest and its proxy surrounding land cover areas. These two multi-band subset images formed each comprised of Blue, Green, Red and Near Infrared bands and they were saved as *.img* files

Image enhancement was carried out in ERDAS IMAGINE through a Radiometric adjustment that effected an equal percentage standard stretch. This was followed by convolution filtering

using a 3x 3 edge enhancement. This was useful in clearly enhancing the area and demarcating the boundaries of Mabira Forest. **Figure 2** and **Figure 3** show the resultant True Colour Composites of these two images while **Figure 4** and **Figure 5** show their resultant False Colour Composites. The Normalised Difference Vegetation Index (NDVI) was then computed for the 2017 and 2019 images as shown in **Figure 1** below.

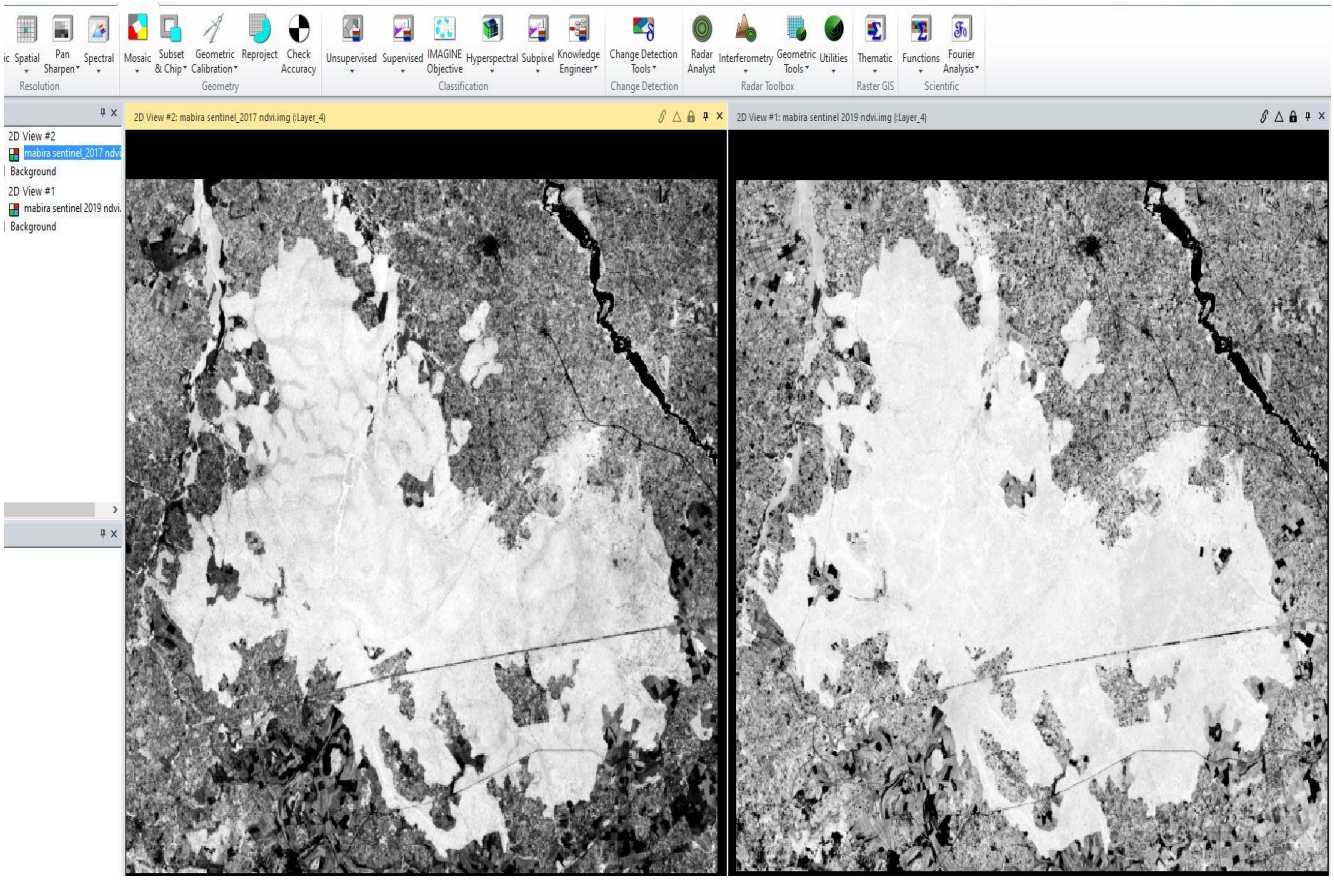

Figure 1: NDVI images for Mabira Forest and its surrounding for 2017(left) and 2019(right).

The extent of Mabira Forest had an average NDVI value of 0.85 in 2017 and 0.75 in 2019 characteristic of evergreen forests. The lower NDVI value in 2019 could be due to increased stress on the forest due to the growing of sugarcane in and around the forest. The surroundings of the forest had NDVI values 0.4 to 0.6 which is characteristic of croplands such as sugarcane and other food crops.

Figure 2: True Colour (Red, Green, Blue) Composite Sentinel-2 subset image of Mabira forest and its surrounding. The image was taken on 25 January 2017. The dark green area is the extent of Mabira Forest. The image has been enhanced using an equal percentage standard stretch and a 3x3 edge enhance, convolution filter.

Figure 3: True Colour (Red, Green, Blue) Composite Sentinel-2 subset image of Mabira forest and its surrounding. The image was taken on 16 March 2019. The dark green area is the extent of Mabira Forest. The image has been enhanced using an equal percentage standard stretch and a 3x3 edge enhance, convolution filter.

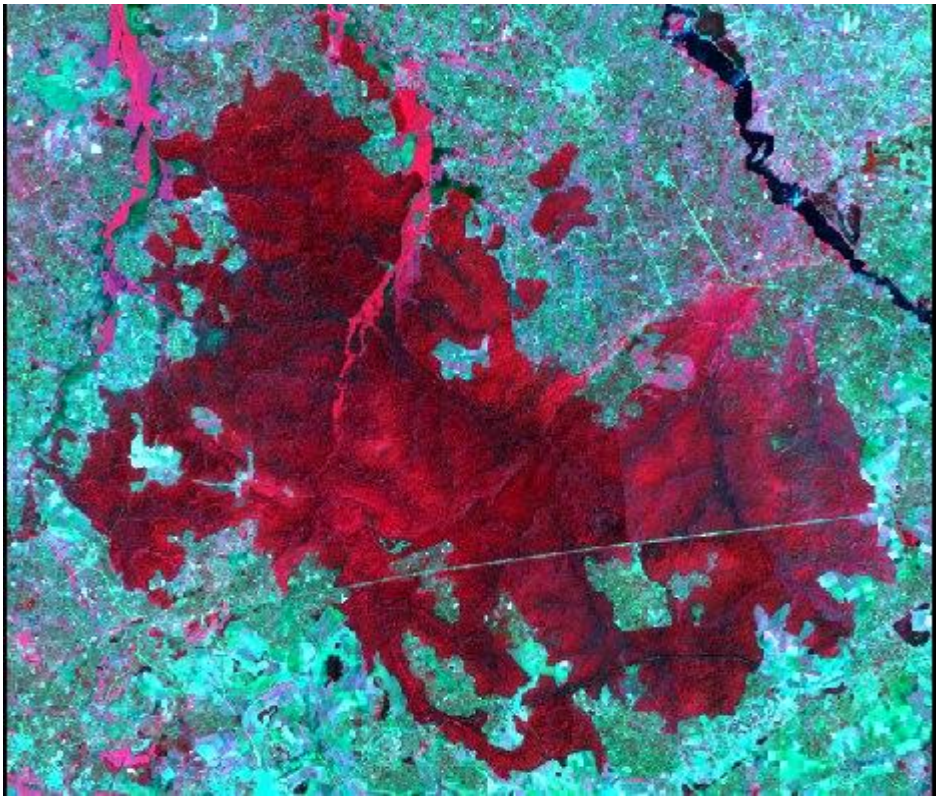

Figure 4: False Colour (NIR, Red, Green) Composite Sentinel-2 subset image of Mabira forest and its surrounding. The image was taken on 25 January 2017. The bright red area is the extent of Mabira Forest. The image has been enhanced using an equal percentage standard stretch and a 3x3 edge enhance, convolution filter.

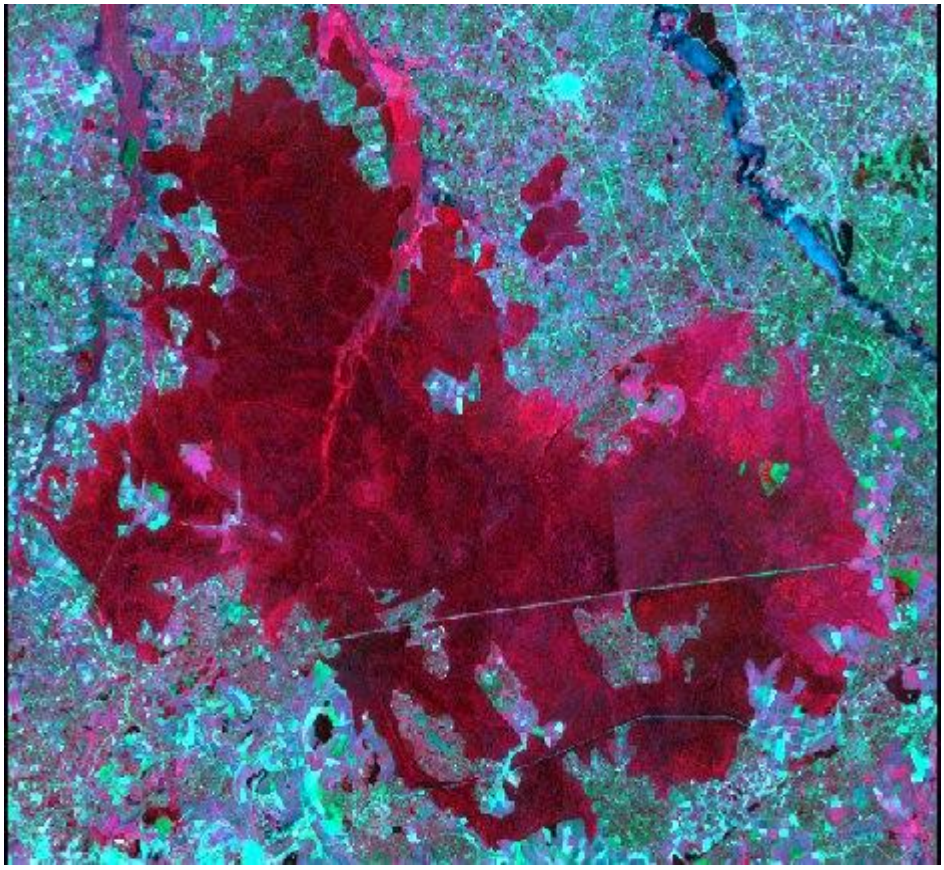

Figure 5: False Colour (NIR, Red, Green) Composite Sentinel-2 subset image of Mabira forest and its surrounding. The image was taken on 16 March 2019. The bright red area is the extent of Mabira Forest. The image has been enhanced using an equal percentage standard stretch and a 3x3 edge enhance, convolution filter.

Supervised Image Classification:

The supervised classification of the 2017 and 2019 sentinel-2 images (**Figure 4 and Figure 5)** to form thematic images (**Figure 6**) consisted of the training, classification, and final output stages. In the training stage, the Sentinel-2 images (**Figure 4 and Figure 5**) were first inspected in ERDAS IMAGINE 2016 and using knowledge of the area in conjunction with GOOGLE EARTH imagery, training sites within the imagery that represents the corresponding areas on the ground were collected. These sites were collected in the form of delineated polygons or representative pixels that ERDAS IMAGINE will use to develop a multiband classification based on spectral relationships scattered from the sites. Each training site represented a homogeneous and contiguous grouping of pixels within an individual category of interest. The number of training sites collected from the imagery captured the amount of variability contained within the category of interest as identified across the entire image data. Also, each training site's category of interest was randomly or systematically distributed throughout the entire image data. In ERDAS IMAGINE, clicking the *Raster* tab, then *Supervised* and *Signature Editor* initiated the training process (Khorram and Nelson, 2019).

In ERDAS IMAGINE, selecting *Raster*, then *Supervised* and *Supervised classification* initiated the classification process (Khorram & Nelson, 2019). The maximum likelihood statistical algorithm was used with these land cover classes; Mature Forest (Dark green), Young Forest (Green), Sugarcane plantation (Cyan), Water (Map grid Blue), Urban developed land (Red), Bare Agricultural land (Yellow). Finally, two thematic images are produced (**Figure 6**).

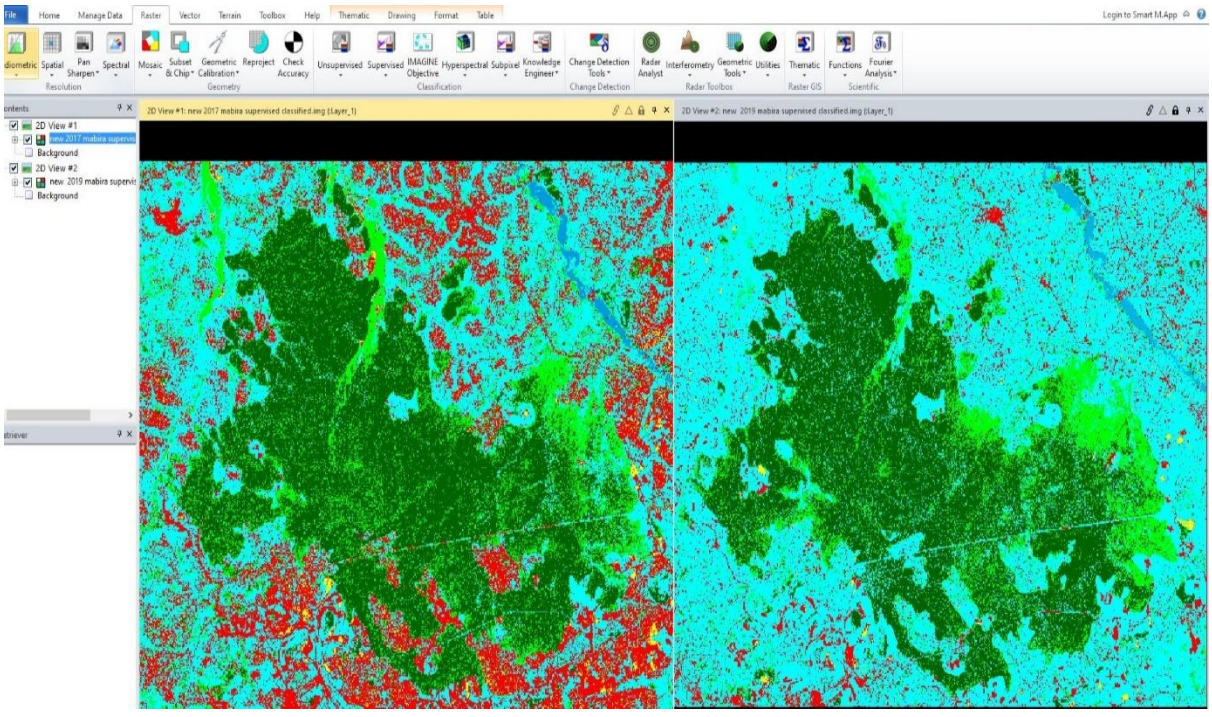

Figure 6: Maximum likelihood Supervised classification images for 2017(left) and 2019(right) showing the land cover and land use classes; Mature Forest (Dark green), Young Forest (Green), Sugarcane plantation (Cyan), Water (Map grid Blue), Urban developed land (Red) and Bare Agricultural land (Yellow). The Maximum likelihood algorithm assumes that the statistical distribution of training data, for each class, and in each band, will follow a normal, Gaussian distribution (Khorram and Nelson, 2019)

Production of Land Cover and Land Use Maps:

Using ArcGIS, two high-resolution, land cover maps were produced. One map shows the land cover for 2017 and the other for 2019. A shape file for districts in Uganda was combined with the thematic images for both 2017 and 2019 to produce the two maps (**Figure 7** and **Figure 8**).

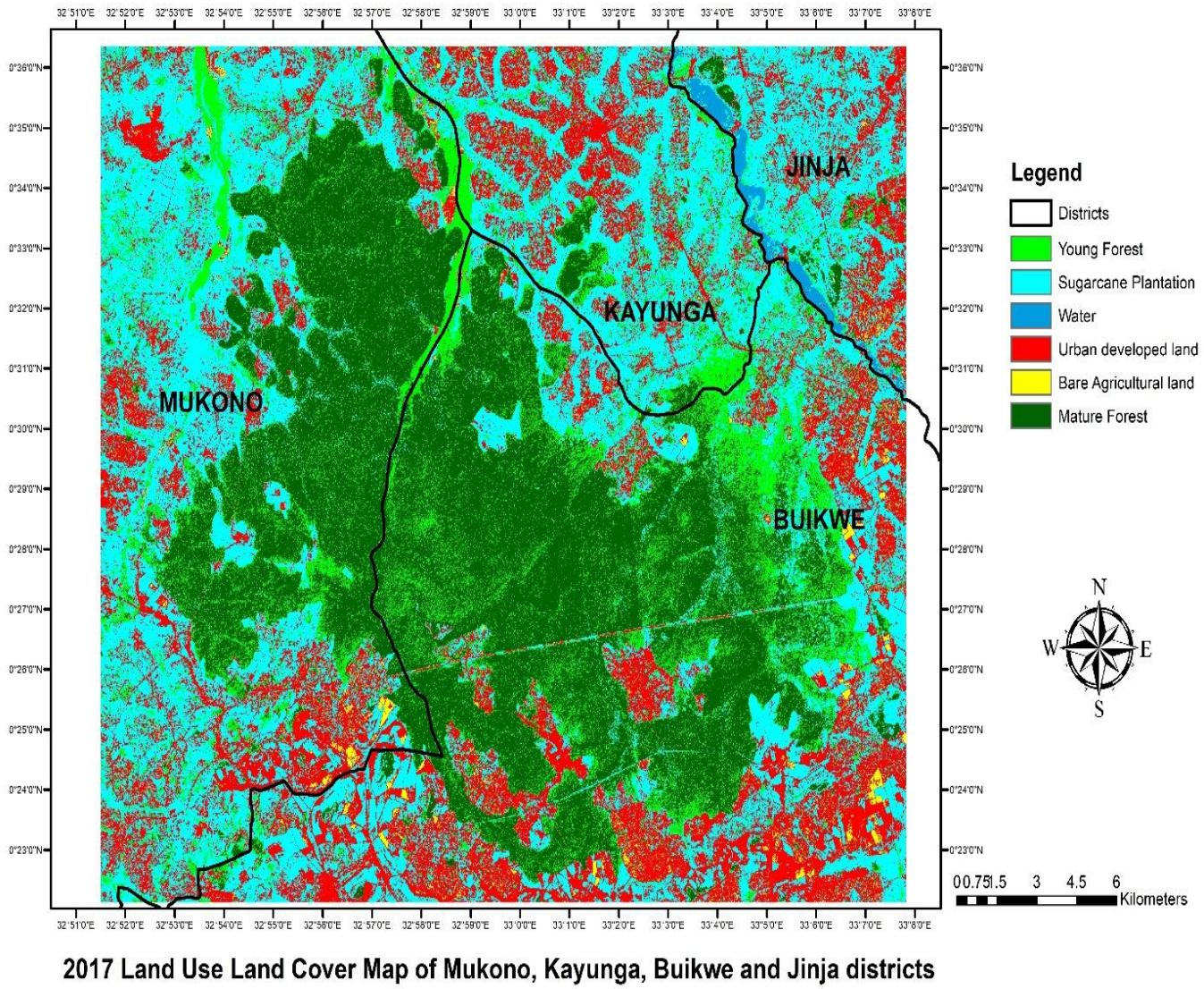

Figure 7: Thematic map showing land cover and land use in and around Mabira Forest in 2017.

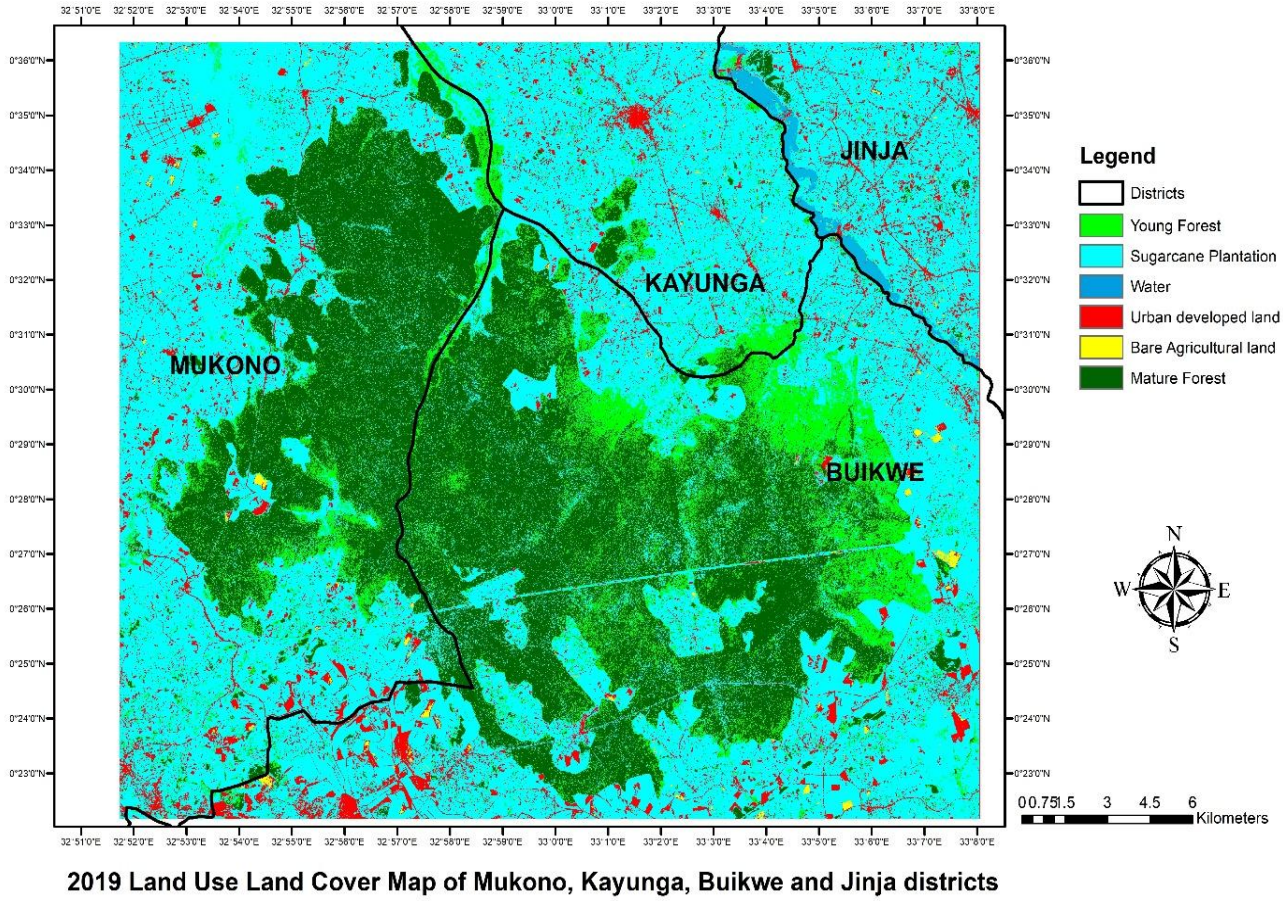

Figure 8: Thematic map showing the land cover and land use in and around Mabira Forest in 2019

Change Detection:

Land cover and land use change detection between 2017 and 2019 was done using an Image Difference operation. This operation subtracted the After Image (the later dated, 2019 classified image) from the Before Image (the earlier dated, 2017 classified image). The output produced two types of image files (**Figure 9**). The first output image file (**Figure 9**) is a grayscale, image difference file that represents the changes in brightness values over time between the before and after classified input images. The second output image file (**Figure 9**) highlights the areas where classes have increased in change (class area) from one image to another, decreased in change from one image to another, or remained unchanged from one image to another (Khorram and Nelson, 2019). The highlighted change areas were specified by a threshold value or percentage as +/− 10% change. In ERDAS IMAGINE, this process was activated by clicking on the *Raster* tab, then *Change Detection Tools*, followed by *Image Difference* (Khorram and Nelson, 2019). Finally, using ArcGIS software, a land cover change map between 2017 and 2019 for Mabira Forest and its environment is produced (**Figure 10**).

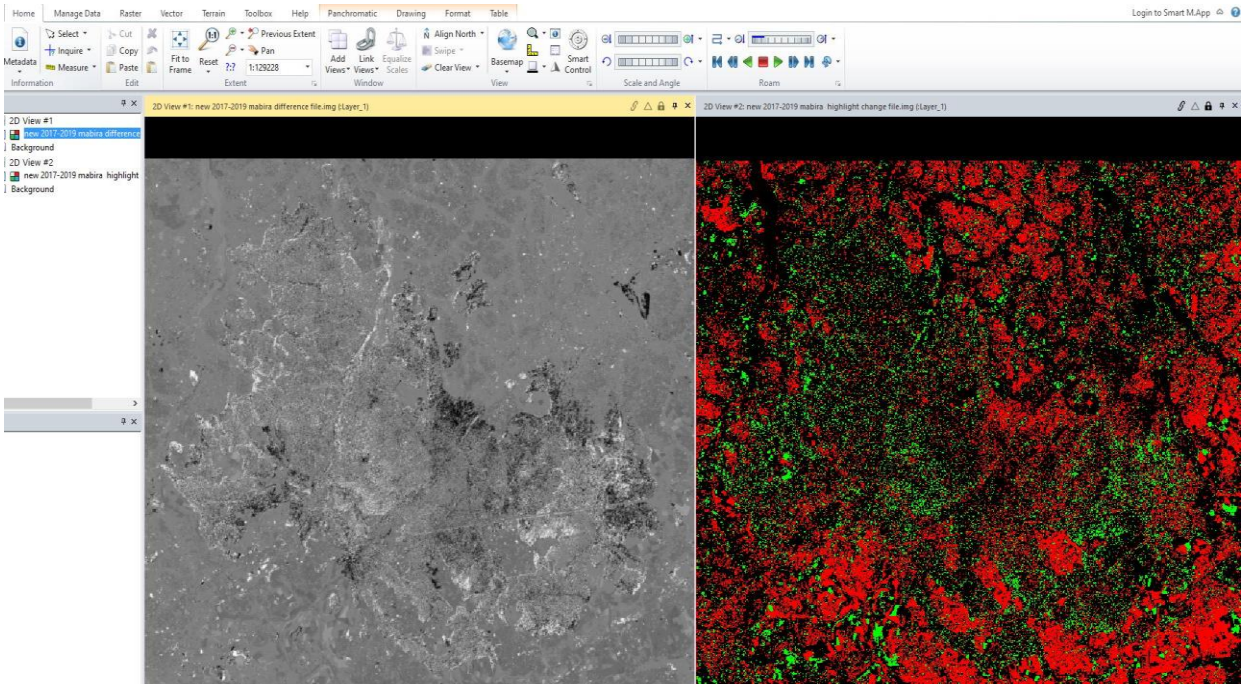

Figure 9: Image Difference File (2D View #1 on left) represents the changes in brightness values over time between the before and after classified input images. Highlight Change File (2D View #2 on right) represents areas that have increased or decreased based on the specified threshold (Green—increases more than 10%, Red—decreases more than 10% and White- No change).

Figure 10: The map below is the corresponding land cover change map for Mabira Forest.

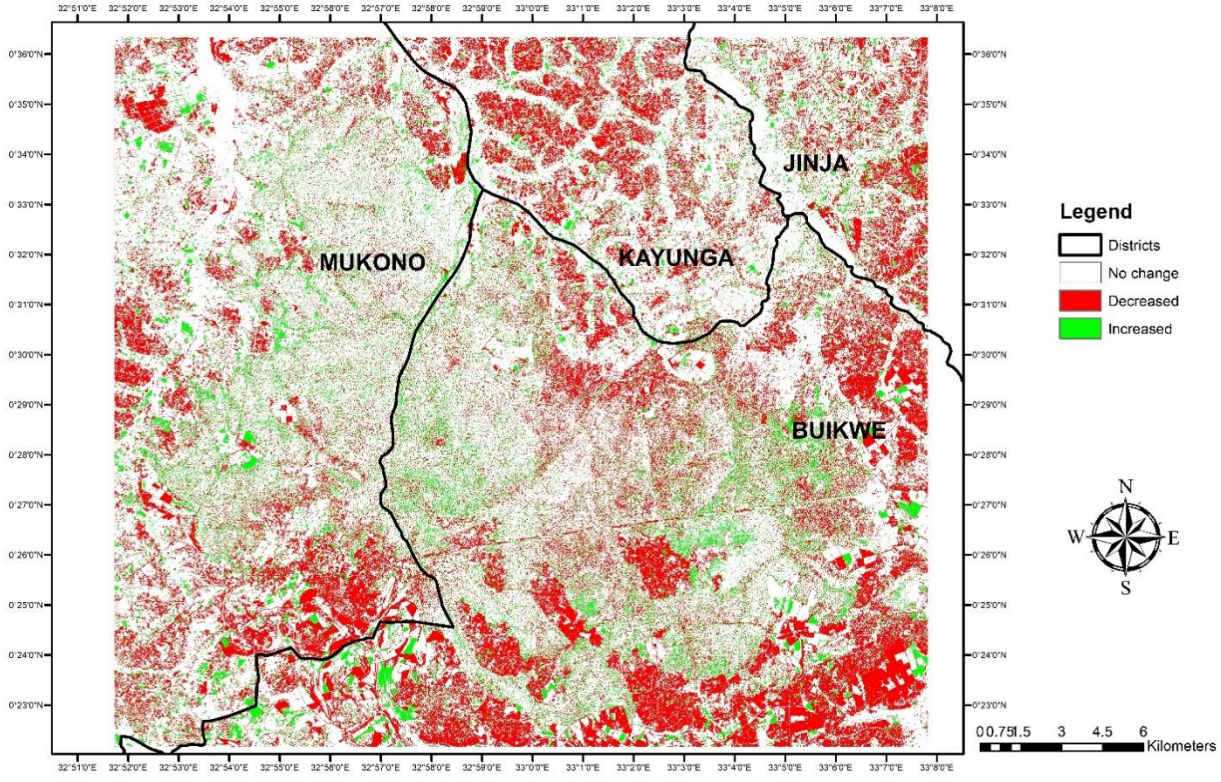

2017 to 2019 Land Cover Change Map of Mukono, Kayunga, Buikwe and Jinja districts

Results and Discussion

Land Cover Transition Matrix:

The land-cover transition matrix was used to compare class value areas between the 2017 Sentinel-2, Mabira Forest thematic image (**Figure 6**: Before Image) and 2019 Sentinel-2, Mabira Forest thematic image (**Figure 6**: After Image). The land-cover transition matrix is useful for determining where land-cover conversions were most prominent (such as the conversion of Forests to Sugarcane plantations), and whether or not all land-cover categories changed. In ERDAS IMAGINE, the land cover transition summary report was generated by clicking on *Raster*, then *Thematic* followed by Summary Report of Matrix (Khorram and Nelson, 2019). From this report, the land cover transition matrix (**Table 2**) shown below was compiled.

2019 / **2017**	**MATURE FOREST** (ha)	**YOUNG FOREST** (ha)	**SUGARCANE PLANTATION** (ha)	**WATER** (ha)	**URBAN DEVELOPED LAND** (ha)	**BARE AGRICULTURAL LAND** (ha)	**TOTAL**
MATURE FOREST (ha)	17989.6 (78%)	2644.8 (11.48%)	2378.8 (10.32%)	0.08 (0%)	28.3 (0.12%)	4.7 (0.02%)	23046 (100%)
YOUNG FOREST (ha)	3186.3 (33.8%)	2895.6 (30.8%)	3221.5 (34.2%)	1.3 (0.01%)	97.8 (1.04%)	5.8 (0.06%)	9408.3 (100%)
SUGARCANE PLANTATION (ha)	953.2 (3.4%)	1286.2 (4.58%)	23621 (84.17%)	56.3 (0.2%)	1957.2 (6.9%)	189.6 (0.68%)	28063 (100%)
WATER (ha)	0.01 (0%)	0.55 (0.12%)	51.95 (10.9%)	416.7 (87.5%)	7.01 (1.48%)	0 (0%)	476 (100%)
URBAN DEVELOPED LAND (ha)	219.5 (1.38%)	380.6 (2.39%)	12717.3 (79.7%)	29 (0.18%)	2502.6 (15.7%)	102.2 (0.64%)	15951.2 (100%)
BARE AGRICULTURAL LAND (ha)	5.18 (0.6%)	27.8 (2.97%)	802.5 (85.6%)	0 (0%)	84.4% (9%)	17.4 (1.86%)	937.2 (100%)
TOTAL	22353.8	7235.6	42793	503.38	4677.3	319.7	

Table 2: Land Cover transition matrix between 2017 and 2019 for Mabira Forest and its surroundings. The two values in the cells are land cover areas in Hectares and land cover areas in percentages (enclosed in brackets) respectively.

Land Cover Area Change between 2017 and 2019:

Table 2 shows land cover area changes for each class. For example, between 2017 and 2019, 2378.8 hectares of Mature Forest were cleared and converted to Sugarcane plantations. This land area accounted for 10.32% of the total area covered by Mature Forest. 28.3 hectares of Mature Forest were converted into urban developed land which accounted for 0.12% of the total area covered by Mature Forest. 4.7 hectares (0.02%) of Mature Forest were converted to other agricultural activities such as the growing of food crops like maize and bananas. 3221.5 hectares (34.2%) of Young Forest were cleared and replaced with sugarcane plantations. 97.8 hectares (1.04%) of Young Forest were converted into urban developed land for settlement and real estate development. 5.8 hectares (0.06%) of Young Forest was converted to agricultural land for the growing of food crops. Clearly, there was a significant loss in the spatial extent of both Mature and Young Forest land cover attributed to mainly sugarcane plantation establishment, urban developed land, and other agricultural activities. The total areas for each land cover class in **Table 2** were utilized to construct **Table 3** below.

LAND COVER	2017		2019		CHANGE (2017-2019)	
	Area(hectares)	Percentage	Area(hectares)	Percentage	Area(hectares)	Percentage
MATURE FOREST	23046	30%	22353.8	28.7%	-692.2	-1.3%
YOUNG FOREST	9408.3	12%	7235.6	9.3%	-2172.7	-2.7%
SUGARCANE PLANTATION	28063	36%	42793	55%	14730	19%
WATER	476	0.6%	503.4	0.6%	27.4	0%
URBAN DEVELOPED LAND	15951.2	20.5%	4677.3	6%	-11273.9	-14.5%
BARE AGRICULTURAL LAND	937.2	1.2%	319.7	0.4%	-617.5	-0.8%

Table 3: Summary of Land cover classes and their respective areas in and around Mabira Forest. The land cover area changes between 2017 and 2017 for each class are displayed in hectares but also as a percentage. Negative values show a decrease in area while the positive ones show an increase.

From **Table 3**, Mature Forest land cover in the districts of Mukono, Kayunga, Buikwe, and Jinja decreased by 1.3% from 30% in 2017 to 28.7% in 2019. Young Forest land cover decreased by 2.7% from 12% in 2017 to 9.3% in 2019. In the same period, the land cover of Sugarcane plantations rose from 36% in 2017 to 55% in 2019. This was a 19% increase. The land cover by water remained constant at 0.6%. Urban developed land reduced by 14.5% and bare agricultural land was reduced by 0.8%. From **Table 2**, we note that 79.7% of urban developed land was reassigned to sugarcane growing while 85.6% of the bare agricultural land was converted to sugarcane growing.

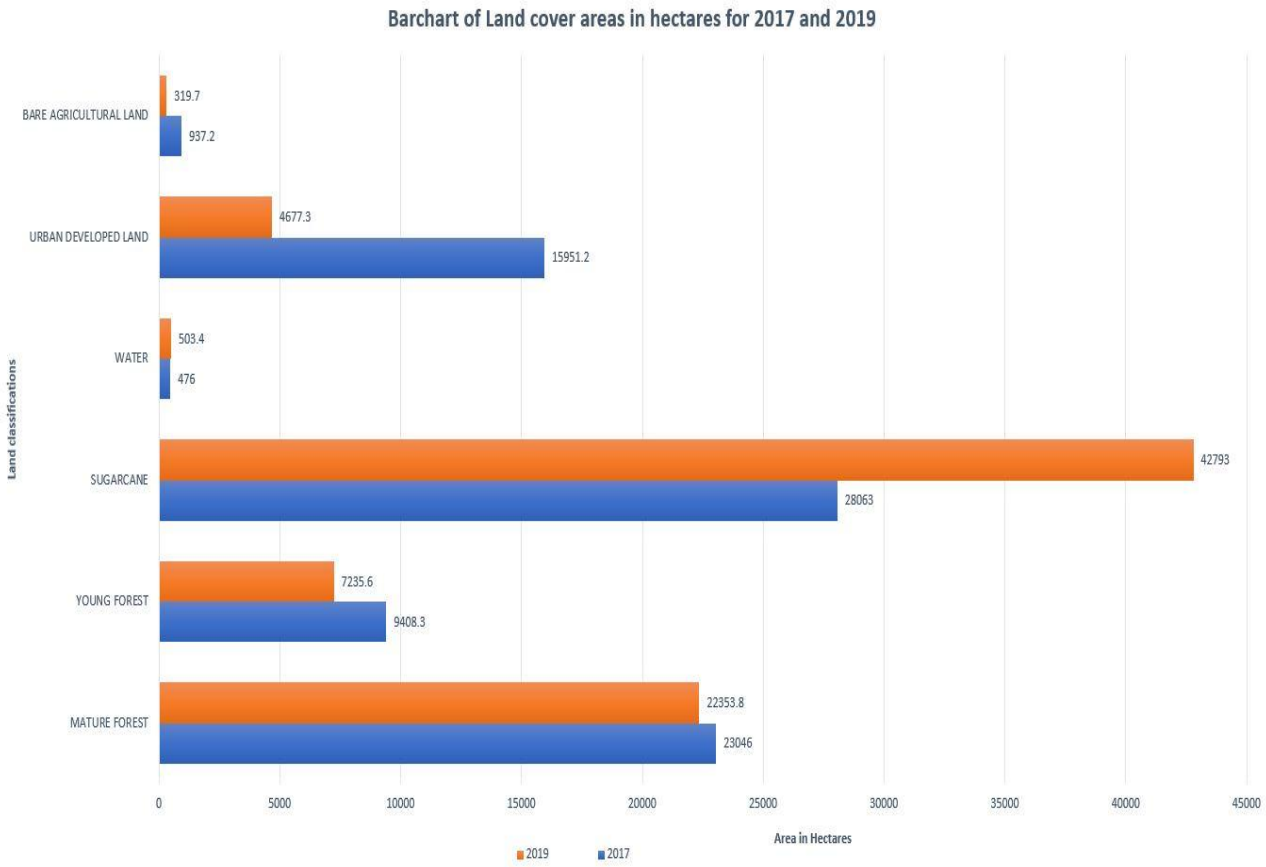

Figure 11: Bargraph showing land cover areas in hectares for 2017 and 2019. The blue colour represents 2017 while the orange represents 2019. The graph shows a 19% increase in sugarcane plantation land cover between 2017 and 2019 at the expense of both Mature and Young Forest land cover.

.

Conclusion

This project has provided empirical evidence(**Table 3**) that a significant amount of forest cover in Mabira Forest was cleared to make way for sugarcane growing between 2017 and 2019. This will eventually impact negatively on climate change and the ecosystem in the forest (Baranga, 2007; Baranga et al., 2013). **Figure 1** provides evidence that the health of the forest deteriorated from an NDVI value of 0.85 in 2017 to 0.75 in 2019 due to growing sugarcane in and around the forest. More stringent protective approaches need to be implemented to mitigate this encroachment.

There is room for improvement of this study by carrying out an assessment of the classification accuracy through the computation of Kappa coefficients, user accuracy and producer accuracy statistics (Mbayaki et al.,2016; Tewabe and Fentahun,2020; Hegazy and Kaloop,2015). This was not done due to time constraints attached to the project life span and the inability of the author to travel and capture GPS primary field data from Mabira Forest in Uganda.

References

Baranga, D., Fungo, B., Eilu, G., and Tweheyo, M. (2013) 'Forest disturbance and cropping mixtures influence crop raiding by red-tailed monkey and grey-cheeked mangabey around Mabira Forest Reserve, Uganda,' *Journal of Ecology and The Natural Environment*, 5(2), pp. 14–23, doi:10.5897/jene11.028.

Baranga, D. (2007) 'Observations on resource use in Mabira Forest Reserve,Uganda', *African Journal of Ecology*, 45(1), pp.2-6

Gomez, C., White, J. C., and Wulder, M. A. (2016). 'Optical remotely sensed time series data for land cover classification: A review.', *ISPRS Journal of Photogrammetry and Remote Sensing*, 116, pp.55–72, doi:10.1016/j.isprsjprs.2016.03.008

Hegazy, I.R. and Kaloop, M.R. (2015) 'Monitoring Urban Growth and land use change detection with GIS and remote sensing techniques in Daqahlia Governorate Egypt', *International Journal of Sustainable Built Environment*, 4(1), pp. 117–124, doi:10.1016/j.ijsbe.2015.02.005.

Khorram, S., and Nelson, S.C. (2019) *Image Processing and Data Analysis with ERDAS IMAGINE*. London : Taylor and Francis Group.

Mbayaki, H., Mubea, K., and Mundia, C. (2016). 'Assessment of Land Use Land Cover Change and Decline in Sugarcane Farming using GIS and Remote Sensing in Mumias District, Kenya', *International Journal of Science and Research*, 5(2), pp 1655-1666

Rawat, J., and Kumar, M. (2015). 'Monitoring land use/cover change using remote sensing and GIS techniques: A case study of Hawalbagh block, district Almora, Uttarakhand, India', *The Egyptian Journal of Remote Sensing and Space Science*, 18(1), pp.77–84, doi:10.1016/j.ejrs.2015.02.002

Tewabe, D. and Fentahun, T. (2020). 'Assessing land use and land cover change detection using remote sensing in the lake tana basin, Northwest Ethiopia', *Cogent Environmental Science*, 6(1), pp.1-11, doi:10.1080/23311843.2020.1778998.